energies

MDPI

Article

An Analysis of the Influence of Low Density Polyethylene, Novolac, and Coal Tar Pitch Additives on the Decrease in Content of Impurities Emitted from Densified Pea Husks during the Process of Their Pyrolysis

Marcin Bielecki, Valentina Zubkova * and Andrzej Strojwas

The Institute of Chemistry, Jan Kochanowski University in Kielce, Uniwersytecka Str. 7, 25-406 Kielce, Poland
* Correspondence: zubkova@ujk.edu.pl

Abstract: The course of pyrolysis of pea husks was studied. It was stated that the compaction of a sample during its pyrolysis causes an almost two-fold increase in the content of hydrocarbons in the composition of volatile products in the temperature range of 350–470 °C. Low density polyethylene (LDPE), novolac, and coal tar pitch (CTP) wastes were added to feedstocks in the amount of 2 wt% in order to decrease the contribution of saturated and unsaturated hydrocarbons along with oxygen-containing compounds in volatile products. The analysis of the obtained products of pyrolysis was conducted using the techniques of thermogravimetry/Fourier transform infrared spectroscopy (TG/FT-IR), attenuated total reflectance (ATR) and ultraviolet (UV)-spectroscopies, gas chromatography-mass spectrometry (GCMS), X-ray diffractions (XRD), scanning electron microscopy (SEM), and energy dispersive X-ray analysis (EDX). It was determined that pitch took the first place in a series of effectiveness in decreasing the content of harmful compounds in pyrolysis products; novolac was the second. A temperature of 370 °C (CTP) lowers the contribution of compounds with carbonyl groups (by approx. 2.7 times) and the contribution of alcohols, phenols, and esters (by approx. 4.4 times). At a temperature of 465 °C, this additive reduces the contribution of saturated and unsaturated hydrocarbons in the composition of volatiles (by approx. 5.8 times) and at a temperature of 520 °C, a more substantial decrease is observed (by approx. 14.3 times). During the pyrolysis in the temperature range of 420–520 °C, LDPE actively emits its own products of decomposition in the form of aliphatic hydrocarbons that negatively affect the environment. The composition of condensed pyrolysis products changes under the influence of additives. In water condensates, the concentration of determined phenols and anhydrosugars increases slightly under the influence of additives. The SEM and XRD investigations proved that inorganics interact with volatile pyrolysis products from the blends of pea husks with additives and change their composition. After the transformation of chemical composition, inorganics catalyse secondary reactions that take place in the pyrolysis products of blends.

Keywords: pyrolysis; biomass; volatile–char interactions

Citation: Bielecki, M.; Zubkova, V.; Strojwas, A. An Analysis of the Influence of Low Density Polyethylene, Novolac, and Coal Tar Pitch Additives on the Decrease in Content of Impurities Emitted from Densified Pea Husks during the Process of Their Pyrolysis. *Energies* **2023**, *16*, 2644. https://doi.org/10.3390/en16062644

Academic Editor: Andrea Reverberi

Received: 11 February 2023
Revised: 6 March 2023
Accepted: 8 March 2023
Published: 10 March 2023

1. Introduction

The formed agricultural wastes can be processed into biofuels. Pea husks belong to such wastes. The Food and Agriculture Organization of the United Nations informs that at present pea ranks second behind the common bean among the most cultivated legumes worldwide. To make transportation and further energy processing easier, these wastes were subjected to densification that is based on their briquetting, tableting, or also pelletizing. In these technological operations, binders of various types were used [1], namely recovered polyvinyl alcohol, waste cooking oil and waste lubricating oil [2], lignin, starch and polyvinyl alcohol [3], xanthan and guar gums [4], pea starch, and carboxymethyl cellulose [5]. The binders for biomass were chosen with regard to the improvement of

strength qualities of the obtained products. For this purpose, Plaza et al. [6] used coal tar pitch (CTP) as an additive to CO_2 adsorbents prepared from pine sawdust pellets. Cheng et al. [7] used coal tar residue as an additive to olive stone biomass. In their opinion, this additive increased the mechanical strength and heating value of pellets. Ioannou and Simitzis [8] and Faliagas et al. [9] proposed to use novolac (NL) in production of carbonaceous adsorbents. Theodoropoulou et al. [10] also added novolac to biomass. However, these authors investigated novolac-resin/biomass composites from the viewpoint of the properties of activated charcoal and their probable use for electrochemical purposes. Thus, the influence of novolac and coal tar pitch on the yield and composition of volatile pyrolysis products has not been studied.

In the last decade, more and more it has been proposed to process biomass with synthetic material wastes such as polypropylene [11], polyethylene terephthalate [12], waste polystyrene foam [13], and polyvinyl chloride [14]. A lot of attention was paid to co-pyrolysis of biomass with polyethylene (PE) due to its smaller residues after pyrolysis compared to other synthetic materials [15–17].

According to several authors [18–23], the presence of PE lowered char yield during its co-pyrolysis with biomass. Zheng et al. [18] suggested that in the case of the blend of pine sawdust with low density polyethylene (LDPE) a decrease in char yield resulted from the occurrence of synergistic reactions between them during co-pyrolysis.

The investigations of the blends of PE with biomass conducted by different researchers revealed a range of contradictions in the results they obtained. According to Hossain et al. [19] and Yang et al. [21], the presence of PE lowered the yield of volatile products during co-pyrolysis with biomass. A different point of view was proposed by Zheng et al. [18] and Tang et al. [22]. Zheng et al. [18] suggested that the addition of LDPE restrains the coking reactions of biomass and causes an increase in the yield of volatile products. Moreover, Tang et al. [22] reported that the yield of gaseous products such as CO, H_2, CH_4, and higher hydrocarbons increased as a result of the interaction of char and LDPE during co-pyrolysis.

However, Xue et al. [23] stated that the co-pyrolysis of PE and red oak limited the amount of CO_2 in gaseous products. The investigations conducted by a range of authors [19–22,24,25] proved that the addition of PE increased the yield of liquid products during co-pyrolysis with biomass. These scientists pointed to the occurrence of the synergistic effect between PE and biomass during co-pyrolysis as a cause of this phenomenon. Lu et al. [20] and Dewangan et al. [25] suggested that such an increase was caused by the transfer of hydrogen from polymer to biomass. Lu et al. [20] and Xue et al. [23] specified that this takes place at the expense of hydrogen transfer from PE to oxygenates originating from biomass. According to Zheng et al. [18], the occurrence of synergistic interactions between pine sawdust and LDPE was caused by the presence of hemicellulose that activated the pyrolysis of LDPE.

Another contradiction referred to the yield of oil. Yang et al. [21] suggested that the greatest yield of oil from the co-pyrolysis of biomass with PE is obtained at the temperature of 600 °C. In turn, Hossain et al. [19] reported that they obtained the greatest yield of oil from the co-pyrolysis of rice straw with PE at the temperature of 450 °C.

According to Yang et al. [21], during three types of co-pyrolysis of LDPE and biomass the content of alcohols and aliphatic compounds in pyrolytic oil increased whereas that of aldehydes, acids, ethers, furans, ketones, phenols, and sugars decreased. Kumagai et al. [24] suggested that the addition of PE to beech wood increased the content of levoglucosan and methoxyphenols in liquid products. According to these researchers, the observed increase in yield was connected with the stabilization of radicals of levoglucosan and methoxyphenols. In their opinion, the stabilization of radicals was caused by the removal of hydrogen from the pyrolysed PE in the gas phase. Summing up, it should be stated that the influence of LDPE additive on the yield and composition of volatile pyrolysis products has not been fully studied despite numerous research.

It follows from the aforementioned that there still exist various contradictions in the field of knowledge about the pyrolysis process of densified biomass with additives. The same relates to how different binders influence the course of the biomass pyrolysis

process—it has not been fully explained and requires additional research. Therefore, this paper is aimed at the investigation of how the additions of LDPE, novolac, and coal tar pitch influence the pyrolytic behaviour of one biomass waste, namely densified pea husks. The specific aims of this research include an analysis of the composition of volatile and condensed pyrolysis products of densified pea husks and their blends with 2 wt.% of additives along with the characteristics of the solid products obtained.

2. Materials and Methods

For research purpose, pea husks (PH) were washed and then dried at room temperature. Next, PH samples were ground to particles of <0.2 mm in size and dried at a temperature of 105 °C. An Elementar Vario Micro Cube CHNS analyser manufactured by Elementar Analysensysteme GmbH (Langenselbold, Germany) was used for elemental analysis of PH samples. The results of this analysis are presented in Table 1.

Table 1. Main characteristics of PH.

Elements	C^d [%]	H^d [%]	N^d [%]	S^d [%]	A^d [%]	%O [a]	HHV [b] [MJ·kg^{-1}]
Amount	40.99 ± 0.28	5.77 ± 0.01	0.03±0.00	0.00	9.59 ± 0.46	43.62% ± 0.23	16.40 ± 0.16

[a] calculated by difference, O [%] = 100 − C^d − H^d − N^d − S^d − A^d; [b] calculated by HHV [MJ·kg^{-1}] = 0.3491 × C^d + 1.1783 × H^d + 0.1005 × S^d − 0.0151 × N^d − 0.1034 × O^a − 0.0211 × A^d. d—dry basis.

The selected inorganic components in the studied PH were determined by the ED-XRF technique. For this purpose, a Niton Goldd+ analyser manufactured by Thermo Fisher Scientific Inc. (Waltham, MA, USA) was used. The results of the analysis are presented in Table 2.

Table 2. The content of selected inorganic elements in studied biomass [mg·kg^{-1}].

Elements	Si	P	S	Cl	K	Ca
Amount	4210 ± 233	233 ± 94	1628 ± 75	475 ± 27	22,343 ± 176	15,052 ± 331

The accuracy of determination was checked on the basis of an analysis of reference materials: NIST-1575a (pine needles), NIST-1573a (tomato leaves), IC-INCT-PVLT-6 (tobacco leaves).

LDPE transparent packaging foil cut into pieces of 1 × 1 mm in size, NL, and a commercial sample of coal tar pitch CTP86BL (CTP) with a softening temperature of 86 °C were used as the additives. The amount of additives was 2 wt.%. The previous studies on solid hydrocarbon feedstocks [26,27] showed that the direction of changes taking place in material during thermochemical treatment can be observed from the amount of 2 wt% of additive. PH sample and its blends with additives were densified to the form of tablets. The tablets of pea husks and blends with additives were obtained in a tablet press using pistons with a diameter of 1.2 cm and 0.8 cm. The density of tablets without additives was 0.955 ± 0.019 g·cm^{-3}, with addition of LDPE-0.954 ± 0.003 g·cm^{-3}, with addition of NL-0.955 ± 0.010 g·cm^{-3}, and with addition of CTP-0.956 ± 0.007 g·cm^{-3}.

The pyrolysis was carried out in a tube furnace PRC 70 × 708/110 M manufactured by Czylok company under a high-purity nitrogen atmosphere to a temperature of 450 °C. The average heating rate was 10 °C·min^{-1}; at the final temperature, the sample was kept isothermal for 30 min to complete the pyrolysis. Next, the heating was turned off and the samples were cooled in nitrogen flow. This experiment was repeated twice for every sample. Information about the mass of studied tablets with a diameter of 1.2 cm and how they are placed in a quartz boat round bottom (100 × 30 × 15 mm) is given in Figure S1 and in Table S1.

The condensates of volatile products were obtained in two ways. Using the first way, the volatile products were passed through a layer of methanol in order to condense polar compounds in it. Using the second way, the volatile products were passed through a layer

of distilled water in order to condense compounds soluble in water. During pyrolysis, methanol and distilled water were cooled with ice water. The yield of methanol and water condensates were determined after evaporation of methanol and water to constant weight.

Additionally, PH samples in loose and densified forms and the samples of densified PH blends with LDPE, NL, and CTP additives were pyrolysed in a Q50 thermobalance (TA Instruments Inc., New Castle, DE, USA) under an atmosphere of high-purity nitrogen. The mass of samples was 20 ± 2 mg. The samples were heated in a standard platinum crucible (100 ul PLATINUM PAN KIT 952018.906). The heating rate was equal to 10 °C·min^{-1}; the heating was carried out up to a temperature of 750 °C. The TGA and DTG curves were registered. The volatile products formed during pyrolysis were transferred through an interface to a Nicolet iS10 spectrometer (Thermo Fisher Scientific Inc., Waltham, MA, USA) and their FT–IR spectra were registered. This experiment was repeated twice for every sample. The obtained FT–IR spectra were next normalised with regard to CO_2 band using an OMNIC9 software. The DTG curves of the loose and densified samples without additives were deconvoluted with an OMNIC9 software. The deconvolution made it possible to determine the contribution of cellulose, hemicellulose, lignin, and extractives, the decomposition of which took part in the formation of this curve [28].

The obtained condensates were studied using a Smart MIRacle module, with which the Nicolet iS10 spectrometer was equipped. The material of condensates was applied on a ZnSe monocrystal. The ATR spectra of samples were registered in the wavenumber range 4000–600 cm^{-1}. This operation was performer three times for every sample. The baseline was corrected in order to eliminate the non-specific background. The registered spectra were normalised with respect to C=C band near 1600 cm^{-1} using an OMNIC9 software according to the methodology described in the work [28].

The samples of condensates of 0.0001 g in weight were dissolved in 50 mL of acetonitrile and studied using a JASCO V630 spectrometer. The UV spectra were registered in the range of 190–360 nm. This operation was performed twice for every sample. The spectra were normalised regarding absorbance at the wavelength of 190 nm using a Jasco Spectra Manager software.

The water condensates were studied using a gas chromatograph QP-2010 Plus (Shimadzu, Kyoto, Japan) coupled with a mass spectrometry detector that was equipped with an HP-5MS column. A quantitative analysis of selected compounds and anhydrosugars was conducted according to the techniques presented in the works [29,30]. The obtained results were calculated per 1 g of samples.

The chars of PH sample and its blends with additives pyrolysed at the temperature of 450 °C were mixed with 10 wt% of NaF as an internal standard. The blends of chars with NaF were studied by X-ray diffraction using an X'Pert Pro MPD diffractometer (PANalytical) equipped with a Cu-anode 1.8. kW X-ray tube with linear exit window. The diffractograms of studied samples were registered using a position sensitive silicon strip detector (X'Celerator) with the dimensions of 15 × 9 mm and 128 strips in 2 Θ angular range from 10° to 45°. The diffractograms were obtained in the mode of U = 45 kV and I = 40 mA.

The chars of the densified samples with and without additives, which were obtained at the temperature of 750 °C, were studied with a Quanta 3D FEG scanning electron microscope manufactured by FEI Company (Hillsboro, OR, USA). The accelerating voltage was 10 keV. An EDX analysis was made during the investigation of these samples, the voltage was 10 keV.

3. Results and Discussion

3.1. Pyrolysis of PH Samples in Loose and Densified Forms

Figure 1 presents the results of a thermogravimetric analysis of PH samples pyrolysed in loose (PHL) and densified (PH) forms.

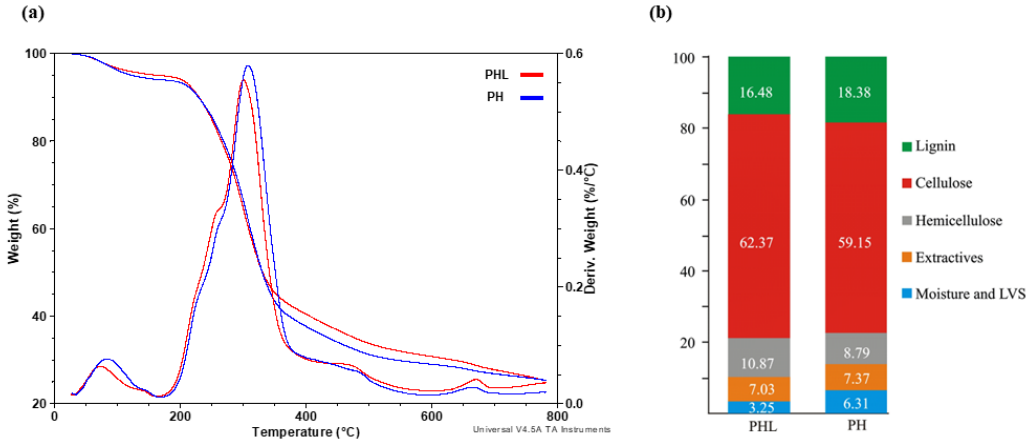

Figure 1. The TGA and DTG curves (**a**) of PHL and PH samples, the deconvolution of DTG curves (**b**); LVS–light volatile species.

The course of the curves in Figure 1a implies that the densification of the PH sample increases the mass loss of sample in the temperature range of 350–750 °C and shifts the maximum in the DTG curve by 7 °C toward higher temperatures. Moreover, densification changes the shape of DTG curves. Such changes indicate alterations in the contribution of biomass components to the formation of the DTG curve. Figure 1b presents the results of deconvolution of the DTG curve. These results imply an increase in the contribution of lignin but a decrease in the contribution of cellulose and hemicellulose in its formation. In turn, this suggests that there are some changes in the thermal stability of these biomass components caused by interactions between them. Thereby, the thermal stability of lignin decreases and that of cellulose and hemicellulose increases under the conditions of densification (Figure 1b). The occurrence of interactions between cellulose and lignin was ascertained in the works [31,32]; the interactions between cellulose and hemicellulose were analysed in the works [33,34]. Liu et al. [33] and Hu et al. [35] pointed out that weak interactions can occur between lignin and hemicellulose.

Figure 2 presents the FT–IR spectra of volatile products obtained from the pyrolysis of loose and densified samples at the temperatures of 370, 470, and 520 °C.

It follows from the comparison of FT–IR spectra in Figure 2 that the densification of the PH sample changes the composition of volatile products of pyrolysis and leads to an increase in the contribution ratio of saturated and unsaturated hydrocarbons, compounds with carbonyl groups, alcohols, and phenols in them. A similar phenomenon of the increasing amount of environmentally hazardous compounds in the composition of volatiles was ascertained during the investigation of a densified sample of soft wood [28]. The changes in composition of the volatile products of pyrolysis can be expected on the basis of data about the composition of condensed products present in them. The ATR spectra of material of the volatile products of pyrolysis of loose and densified PH samples condensed in methanol are presented in Figure 3.

The normalised ATR spectra of condensates in Figure 3 imply that the densification of the PH sample causes an increase in the contribution ratio of the compounds able to form hydrogen bonds and bonds of the C_{al}–H type. In the condensates from densified samples, there is an increase in the contribution of the compounds with carbonyl groups and ester bonds, alcohols, phenols, and compounds with out-of-plane C_{ar}–H bending vibration. This implies that the densification of the PH sample not only increases the yield of volatile components (Figure 2) but, also, enhances the contribution of environmentally hazardous compounds in them. Further research was conducted in an attempt to reduce the emission of harmful compounds during the pyrolysis of the densified PH samples.

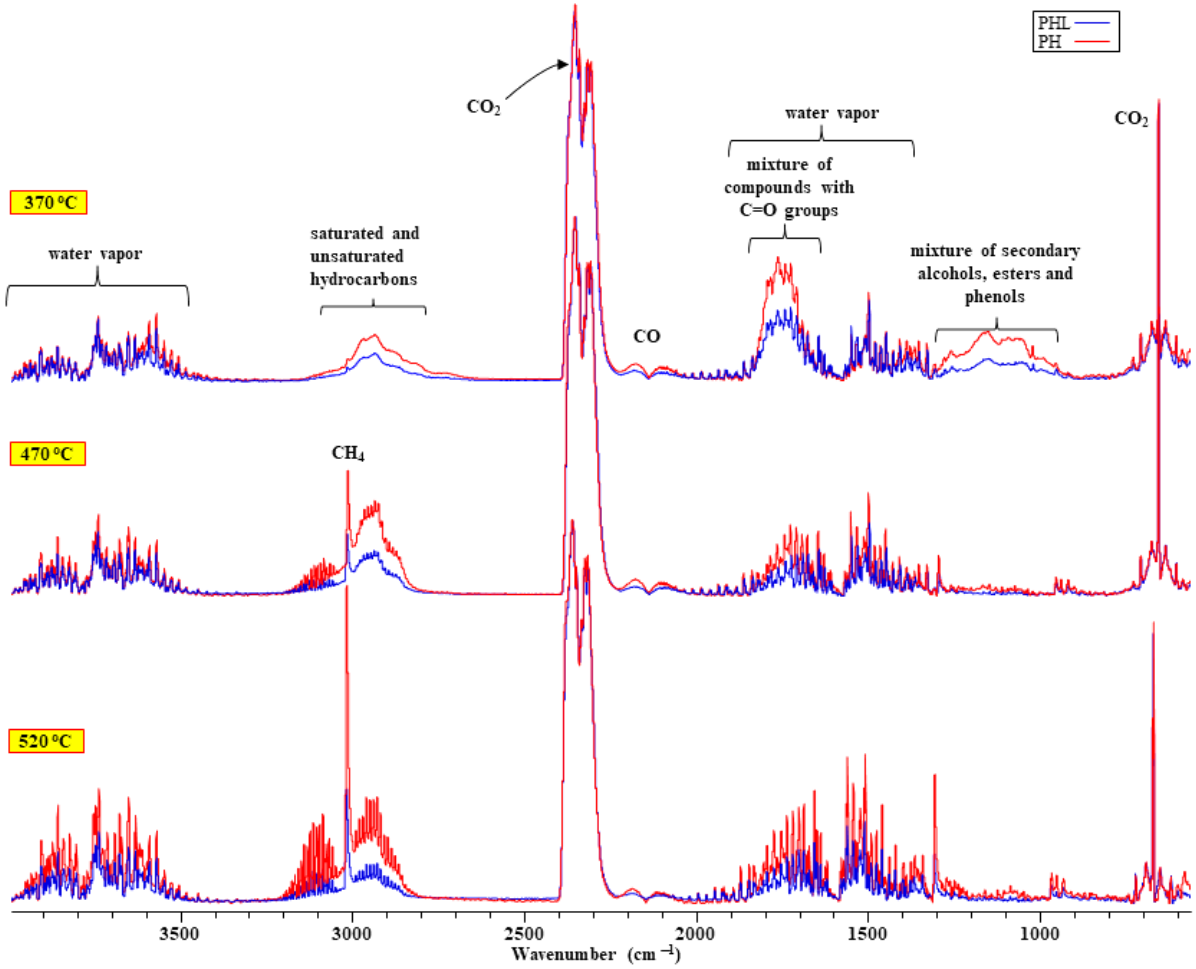

Figure 2. The volatile products of pyrolysis of PH samples in loose and densified forms.

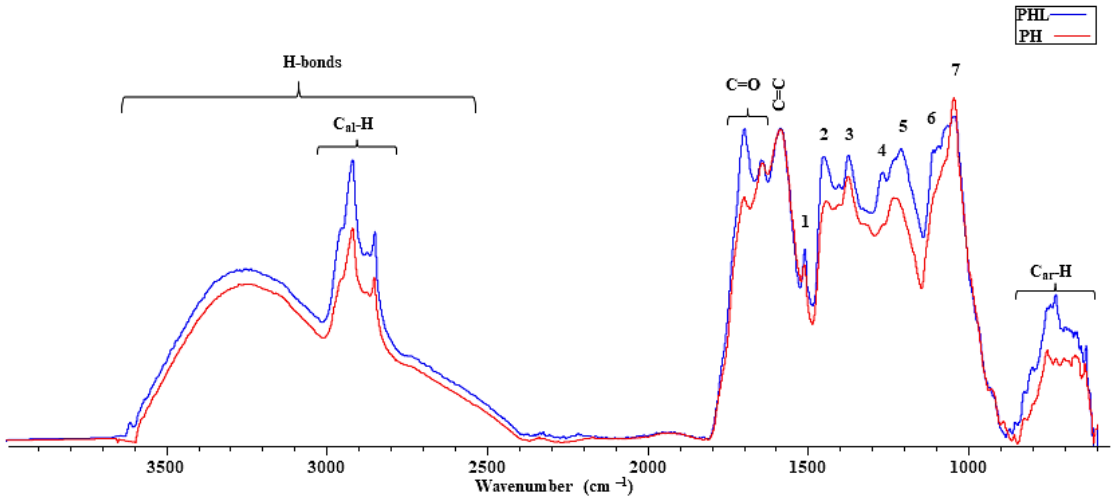

Figure 3. The ATR spectra of condensates from PH samples pyrolysed in loose and densified forms. (1) aromatic skeletal vibrations in fragments with guaiacyl rings; (2) C–H asymmetric deformation of $–OCH_3$, CH_2 in pyran ring symmetric scissoring; (3) C–H deformation in fragments of hemicellulose, (4) C–O stretching in lignin, C-O linkage in guaiacyl aromatic methoxyl groups; (5) C–O stretching in syringyl rings, (6) C–H vibrations in lignin; (7) C–O stretching in fragments of cellulose and lignin [36,37].

3.2. Pyrolysis of PH Samples with CTP, NL, and LDPE Additives

Figure 4 presents the results of thermogravimetric analysis of the densified PH sample and its blends with CTP, NL, and LDPE additives.

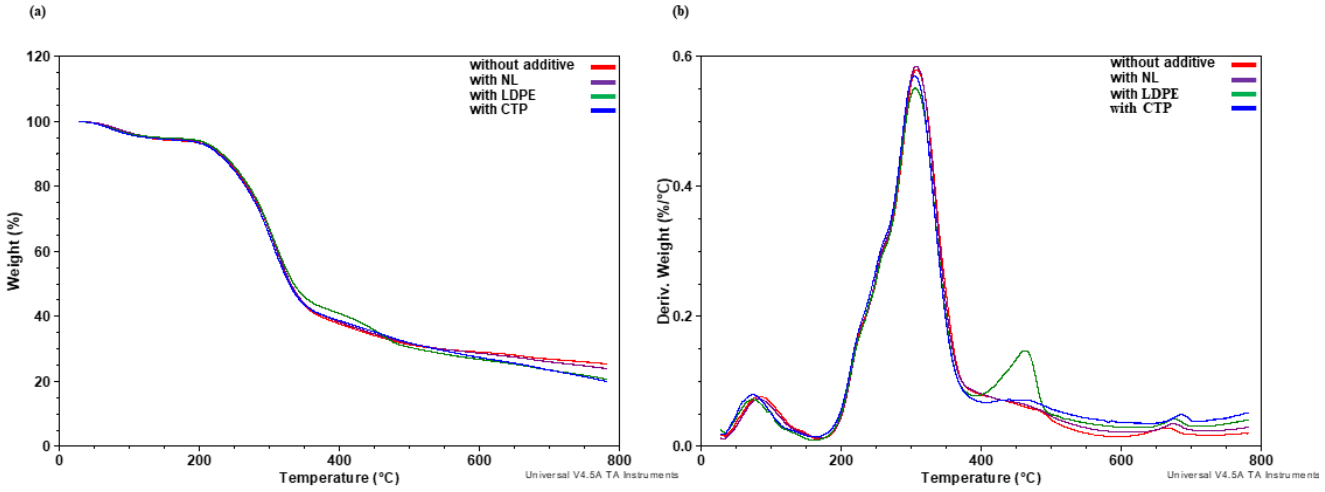

Figure 4. The TGA (**a**) and DTG (**b**) curves of volatiles of densified PH sample and PH blends with additives.

It follows from the comparison of shapes of TGA and DTG curves in Figure 4 that the additives do not change their shape in the temperature range below 500 °C. The only exception is the course of curves of PH blend with LDPE. The deviation of the TGA curve of the PH blend with LDPE from the course of other curves at temperatures of 350–450 °C implies the lack of depolymerization of LDPE at these temperatures in the blend with the PH. The depolymerization of LDPE takes place near 462.3 °C which is evidenced by a peak in the DTG curve. It was noticed in the works by other authors [38–40] that at this temperature an intensive depolymerization of LDPE takes place. Xiong et al. [16] suggested that a decrease in the mass loss before depolymerization of HDPE takes place as a result of persistence of volatiles from biomass in melting polymer.

The deviations in the course of the TGA and DTG curves of densified PH blends with additives regarding that of the densified PH sample are observed in the temperature range of 500–750 °C (Figure 4). This implies a possible occurrence of interactions between volatile products of pyrolysis and char which was reported in works by many authors [41–43]. In the temperature range of 650–700 °C, there is a visible peak in the DTG curve. Its presence can be caused by the changes in composition of the volatile products of pyrolysis as a result of secondary reactions in the gas phase [44,45]. It cannot be excluded that the appearance of this peak is caused by the interactions between volatiles that changed composition and the surface of formed char.

The increase in yield of volatiles during the co-pyrolysis of densified PH sample with additives raises a question about the presence of condensed products in these volatiles. Table 3 presents the yields of condensates obtained at the cooling of volatiles during the pyrolysis of the densified PH sample and its blends with additives.

Table 3. The yields of material soluble in methanol and water [wt%].

Samples	Material Condensable in Methanol	Material Condensable in Water
PH without additive	0.87 ± 0.07	0.76 ± 0.04
PH with NL	1.39 ± 0.09	1.32 ± 0.07
PH with CTP	1.65 ± 0.11	1.52 ± 0.13
PH with LDPE	1.67 ± 0.02	1.08 ± 0.03

It follows from the data in Table 3 that all additives in the blend with PH increase the yields of condensates. Other scientists in their works [19,21,24] drew attention to the increase in yields of liquid pyrolysis products under the influence of PE. This increase in yield of condensates points to the occurrence of interactions between additives and the material of PH at temperatures below 450 °C. Moreover, it implies that greater amounts of condensable compounds can be a result of secondary reactions between the volatile products of PH destruction and the volatile compounds originating from additives. The possibility of secondary reactions in the volatile phase was reported in the works [44,45].

In light of the above considerations, it was reasonable to compare structural-chemical parameters of the obtained condensates, the ATR spectra of which are presented in Figure 5.

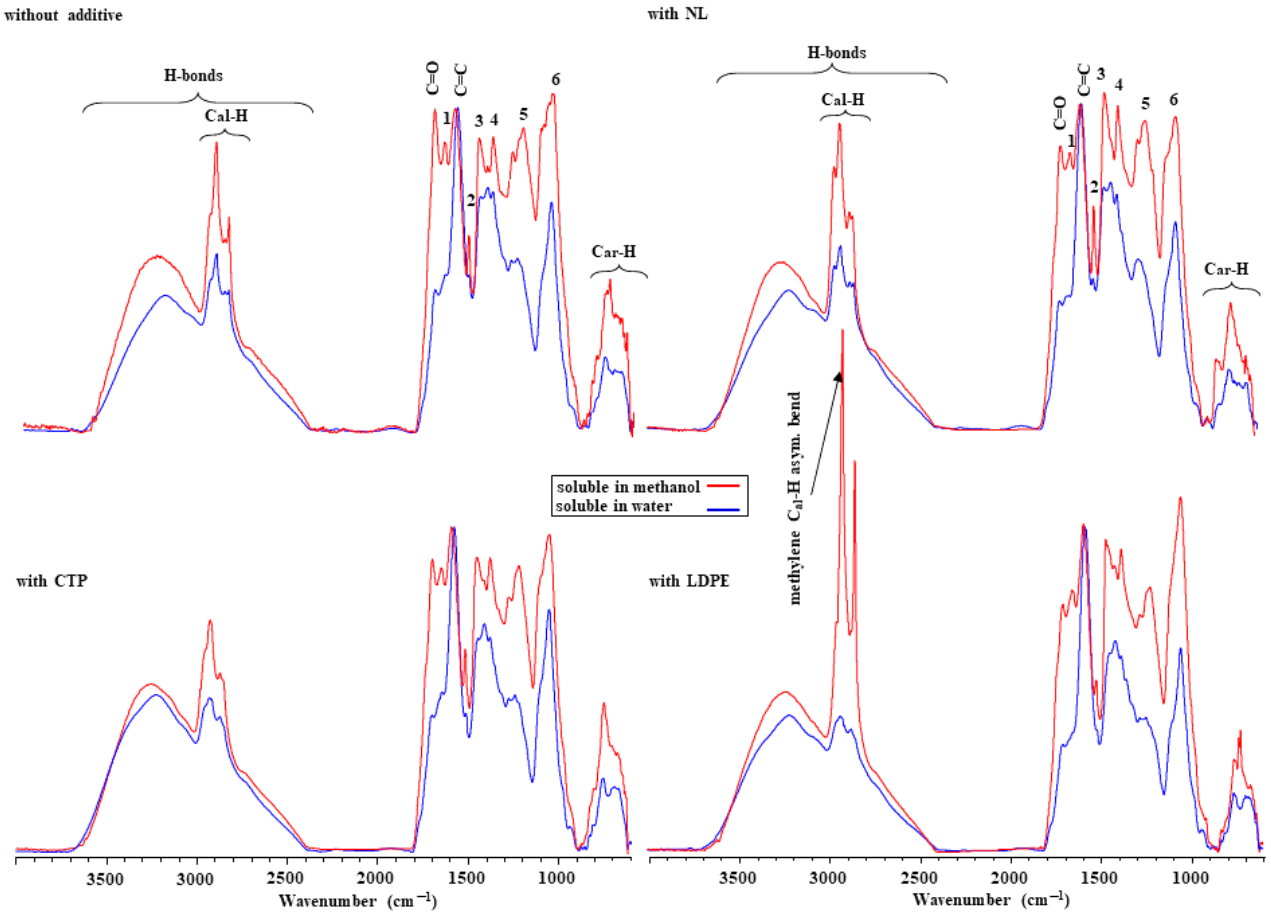

Figure 5. The ATR spectra of condensed material. (1) vibrations of esters, ketones, and aldehydes; (2) aromatic skeletal vibrations in fragments with guaiacyl rings; (3) C–H asym. deformation of $–OCH_3$, CH_2 in pyran ring symmetric scissoring; (4) C–H deformation in fragments of hemicellulose; (5) C–O stretching in syringyl rings; (6) C–O stretching in fragments of cellulose and lignin [36,37].

It follows from the comparison of shapes of the normalised FT–IR spectra of methanol and water condensates in Figure 5 that all condensates have compounds with similar functional groups in their composition but the concentration of these groups in condensed material is different. In the water condensates, there is small contribution of compounds with carbonyl groups and aromatic skeletal vibrations in fragments with guaiacyl rings. The contribution of compounds able to form hydrogen bonds (the range of 3680–2400 cm^{-1}) lowers substantially in the water condensates, the absorbance of all bands diminishes in the wavenumber range of 1500–600 cm^{-1}. In the material that is soluble in methanol the height of the bands of the bonds of C_{al}-H type changes under the influence of CTP and LDPE. Under the influence of CTP the height of methylene C_{al}-H asym. bend decreases by 1.26 times whereas under the influence of LDPE it increases by 1.72 times compared to

this band of the methanol condensate from the sample without additives. In the methanol condensates, NL and LDPE additives lower the contribution of compounds having deformation vibrations of C_{ar}–H type in the wavenumber range of 900–600 cm^{-1} compared to the condensate of the sample without additives. There are distinct contributions of compounds with chromophore groups in the composition of the condensed material. Such distinctions show that the used additives change the composition of the condensed material in different ways.

Figure 6 presents a comparison of the normalised UV spectra of condensates.

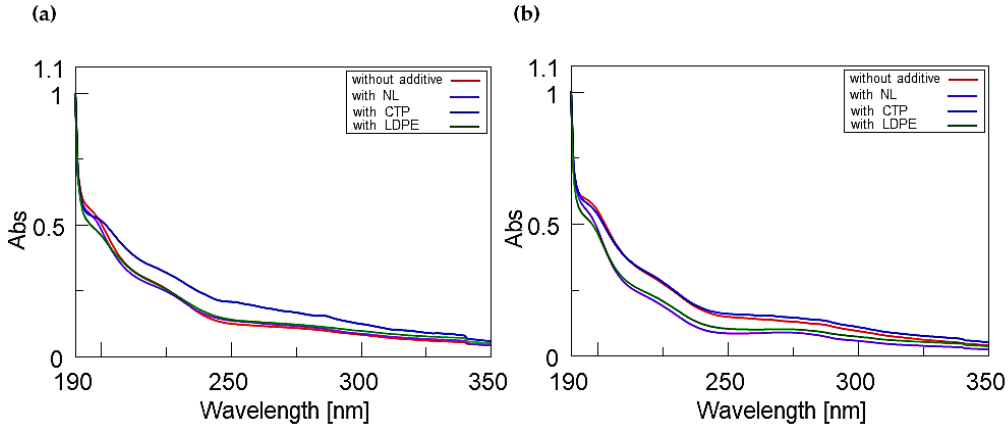

Figure 6. The UV spectra of methanol (**a**) and water (**b**) condensates.

It follows from the shape of the UV spectra in Figure 6a that only the CTP additive causes an increase in absorbance of the material that is soluble in methanol. The spectrum of methanol condensate in Figure 6a is located above the other spectra. This suggests that there is a greater amount of compounds with chromophore groups in this condensate. Figure 6b presents the UV spectra of water condensates. Among water condensates, the condensates from the densified PH sample and its blend with CTP possess unsaturated compounds with chromophore groups most of all. The differences in the composition of condensed material imply that the composition of volatile products of pyrolysis of the densified PH sample and its blend with additives can also differ.

Table 4 presents the values of the concentration of selected carboxylic acids and anhydrosugars determined in the water condensates during the pyrolysis of the PH sample and its blend with additives calculated per 1 g of pyrolysed samples.

Table 4. The concentration of selected organic compounds present in the water condensates [mg/L].

Samples	Carboxylic Acids			Anhydrosugars		
	CH_3COO^-	$HCOO^-$	$C_2O_4^{2-}$	LG	MN	GA
without additives	116	5.3	<0.01	0.13	0.16	0.07
with NL	123	5.7	<0.01	0.17	0.22	0.13
with CTP	119	5.6	<0.01	0.20	0.23	0.13
with LDPE	123	5.8	<0.01	0.16	0.08	0.10

LG—levoglucosan; MN—mannosan, GA—galactosan.

It follows from the data in Table 4 that all additives to the PH sample cause a slight increase in the concentration of carboxylic acids and anhydrosugars in the composition of water condensates. LDPE additive decreases the concentration of MN and GA compared to the concentration of these components in the condensate of the sample pyrolysed without additives. A similar situation is observed for the concentration of determined phenols in the water condensates of the PH sample but these changes are not significant (Table S2).

Figure 7 presents a comparison of the normalised FT–IR spectra of volatile products of the densified PH sample with and without additives.

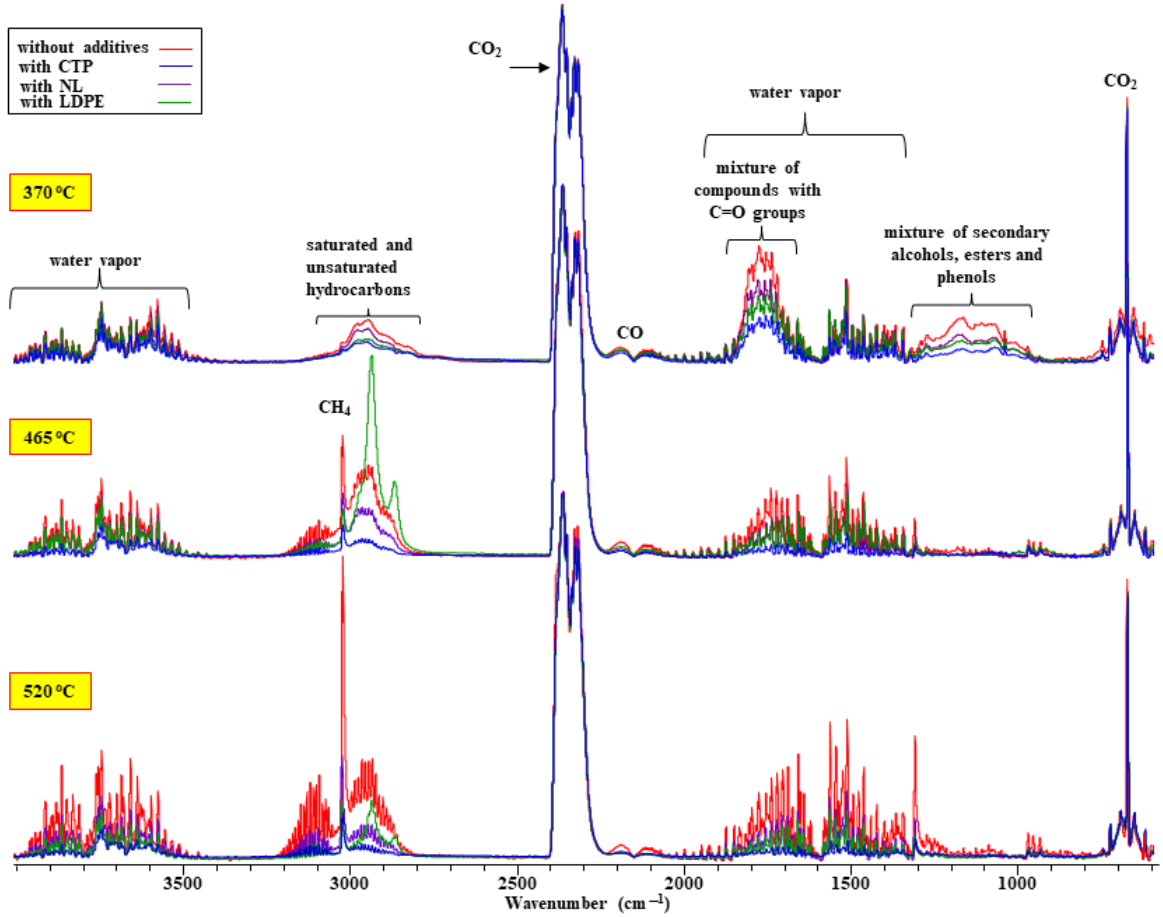

Figure 7. The FT–IR spectra of volatile products of pyrolysis.

It follows from Figure 7 that CTP and NL additives lower the yield of undesirable compounds in the composition of volatile products in the whole temperature range of pyrolysis. The blend of the PH sample and LDPE behaves differently. It is clearly visible in the FT–IR spectra (at a temperature of 370 °C) that the contribution of compounds with carbonyl groups (aldehydes, carboxylic acids, ketones, esters, alcohols, and phenols) in the composition of volatiles decreases under the influence of additives. At a temperature of 462 °C, at which the maximum of mass loss rate is observed, LDPE actively undergoes depolymerization [18–20]. In the FT–IR spectra, at a temperature of 465 °C, there appears a distinct band that points to the emission of products of this decomposition. The products of decomposition of LDPE are still visible at a temperature of 520 °C. This gives good reasons to conclude that during the co-pyrolysis of the PH sample and LDPE there can occur some interactions between the products of depolymerization of LDPE and char in the PH sample.

Table 5 presents the calculations of the surface area ratios of the bands in the FT–IR spectra of volatile products of the PH sample without additives with respect to the appropriate parameters of the samples with additives.

The FT–IR spectra presented in Figure 7 and the results in Table 5 indicate that CTP additive decreases the contribution of undesirable compounds in the composition of volatile products of pyrolysis of PH to a greater extent than NL and LDPE additives. At a temperature of 370 °C, CTP additive lowers the contribution of compounds with carbonyl groups by 2.70 times and the contribution of alcohols, phenols, and esters by 4.38 times. At a temperature of 465 °C, this additive reduces the contribution of satu-

rated and unsaturated hydrocarbons in the composition of volatiles by 5.75 times and by 14.25 times at the temperature of 520 °C.

Table 5. The surface area ratios of the bands in the FT–IR spectra of volatile products of pyrolysis of PH sample and its blends with additives.

Samples	370 °C		465 °C	520 °C
	$A_{C=O\ PH}/A_{C=O\ with\ add}$	$A_{alc\text{-}phen\ PH}/A_{alk\text{-}phen\ with\ add}$	$A_{HC\ PH}/A_{HC\ with\ add}$	$A_{HC\ PH}/A_{HC\ with\ add}$
With NL	1.39 ± 0.02	1.75 ± 0.02	1.92 ± 0.03	2.85 ± 0.04
With CTP	2.70 ± 0.13	4.38 ± 0.18	5.75 ± 0.19	14.25 ± 0.47
With LDPE	1.64 ± 0.02	2.19 ± 0.02	0.92 ± 0.01	3.56 ± 0.01

$A_{c=O}$—surface area of band that corresponds to compounds with carbonyl groups. $A_{alc\text{-}phen}$—surface area of band that corresponds to alcohols, phenols, and esters. A_{HC}—surface area of band that corresponds to hydrocarbons.

Summarizing the above, it should be noticed that the interactions between the PH sample and the additives took place at temperatures below 450 °C which is evidenced by the FT–IR spectra of volatile products. At temperatures above 500 °C, in turn, the secondary reactions, on which the additives also may exert influence, can take place. These reactions can occur not only in the gas phase [44,45] but, also, as a result of the interactions between the volatile products and formed chars [41,43,46]. These considerations follow from an analysis of the thermogravimetric curves in Figure 3. In order to analyse the influence of additives on the structure and composition of chars, their diffractograms were compared in Figure 8.

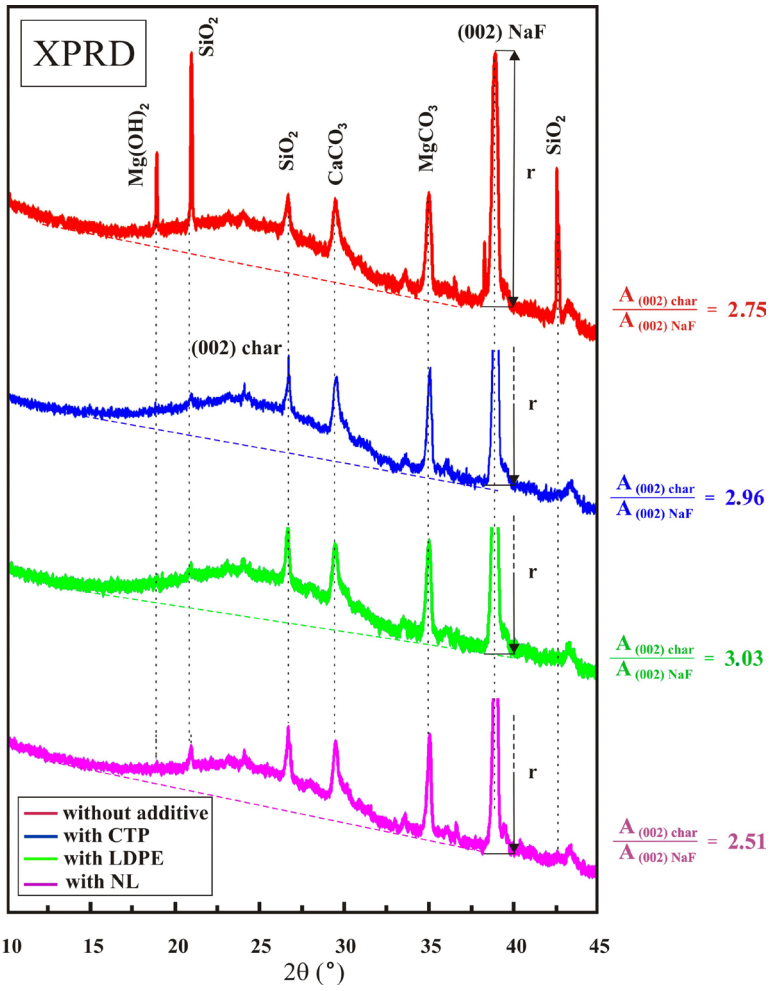

Figure 8. The diffractograms of chars of densified PH sample and its blends with additives that were pyrolysed to a temperature of 450 °C.

The diffractograms in Figure 8 were normalised with respect to (002) reflex from the internal standard NaF; the ratios of surface areas of (002) reflexes of chars and NaF were determined. The ratio of the surface area of the char of the PH sample without additives ($A_{(002)char}/A_{(002)NaF}$) was equal to 2.75; the parameters of appropriate ratios for the char of PH sample with NL were 2.51; for the char with LDPE, it was 3.03 and for the char with CTP, it was 2.95. Different values of the ratios show that the interactions with the volatile products in the chars of studied samples influenced the changes in the amount of carbon atoms that participate in the processes of coherent X-ray scattering. Therefore, the diffractograms presented in Figure 8 imply that the degree of the ordering of C atoms in chars increases under the influence of interactions of the PH sample with LDPE and CTP but decreases under the influence of NL.

Attention should be drawn to the fact of the presence of reflexes from inorganic components in the diffractograms. The reflexes from $Mg(OH)_2$ near 2Θ 18.7 angle and those from SiO_2 near 2Θ 20.7, 38.0, and 42.3 angles are present in the diffractograms of the PH sample without additives. These reflexes do not occur in the diffractograms of the PH samples with additives. It suggests that during the pyrolysis of the PH sample with additives in the medium of the volatile products with a different composition these compounds are not present. The lack of the aforementioned reflexes in the diffractograms of chars with additives gives reason to suggest that $Mg(OH)_2$ undergoes decomposition with the formation of MgO. MgO is probably reduced to metallic Mg at an increased temperature and the aggressive medium of the volatile products of the pyrolysis of the PH sample with additives [47]. However, SiO_2 crystals are reduced from the formed Mg to powdered Si [48] with the formation of MgO, etc. This way, the additives not only change the composition of the volatile products of pyrolysis but, also, cause changes in the structure and composition of the char itself. The height of the reflexes of $CaCO_3$ and $MgCO_3$ in the diffractograms of additives is almost the same. According to Shen et al. [49], $CaCO_3$ and $MgCO_3$ can effectively modify the yield and composition of pyrolysis products. If their content in chars is equal, it can be expected that their influence on the structure of char and the composition of volatiles will be the same. The diffractograms in Figure 8 and the FT–IR spectra in Figure 7 contradict such expectations. This fact implies that volatile products interact with the inorganic components of chars in other ways that are not observable in the diffractograms. Figure 9 presents a visualization of chars pyrolysed to a temperature of 750 °C.

In Figure 9a–d, a comparison of the SEM images made at the magnification of M300 showed the presence of crushed pieces of chars having different shapes: There are visible rod-shaped objects and irregularly shaped objects with a flat surface. There are some brick-shaped objects visible on the surface of some 'rods' (Figure 9e–h). The surface of rods has a distinct relief: the material of 'bricks' from the PH sample without additives has a greater compactness, the 'bricks' material surface from the PH sample with NL looks degraded, the 'bricks' surface from the PH sample with CTP looks as if there were deposits of other material, and the material of 'rods' from the PH sample with LDPE is crumbled to such great extent that in some spots the edges of 'bricks' are invisible. The EDX point microanalysis of 'bricks' showed the presence of great amounts of Ca and O atoms and smaller amounts of K, C, and Cl atoms in their composition (Table S3). The XRD data (Figure 8) imply that there is mostly $CaCO_3$ present in them. The interactions of $CaCO_3$ with the volatile products of decomposition of the PH sample with additives as ligands may cause the differences in composition of the material of 'bricks' and the formation of their complexes [50]. It cannot be excluded that in the presence of Mg^{2+} ions there can be complex calcium carbonate aggregates formed that have the morphology and texture similar to the morphology of aggregates presented in the work by Huang et al. [51]. Attention should be drawn to the fact that the amount of C atoms on the surface of 'bricks' with CTP is slightly larger than in the case of the blends with NL and LDPE. It can only be presumed that this may be caused by a greater amount of aromatic hydrocarbons in CTP

that can interact with $CaCO_3$ as ligands and form the deposits with a greater amount of C atoms on the surface of 'bricks'.

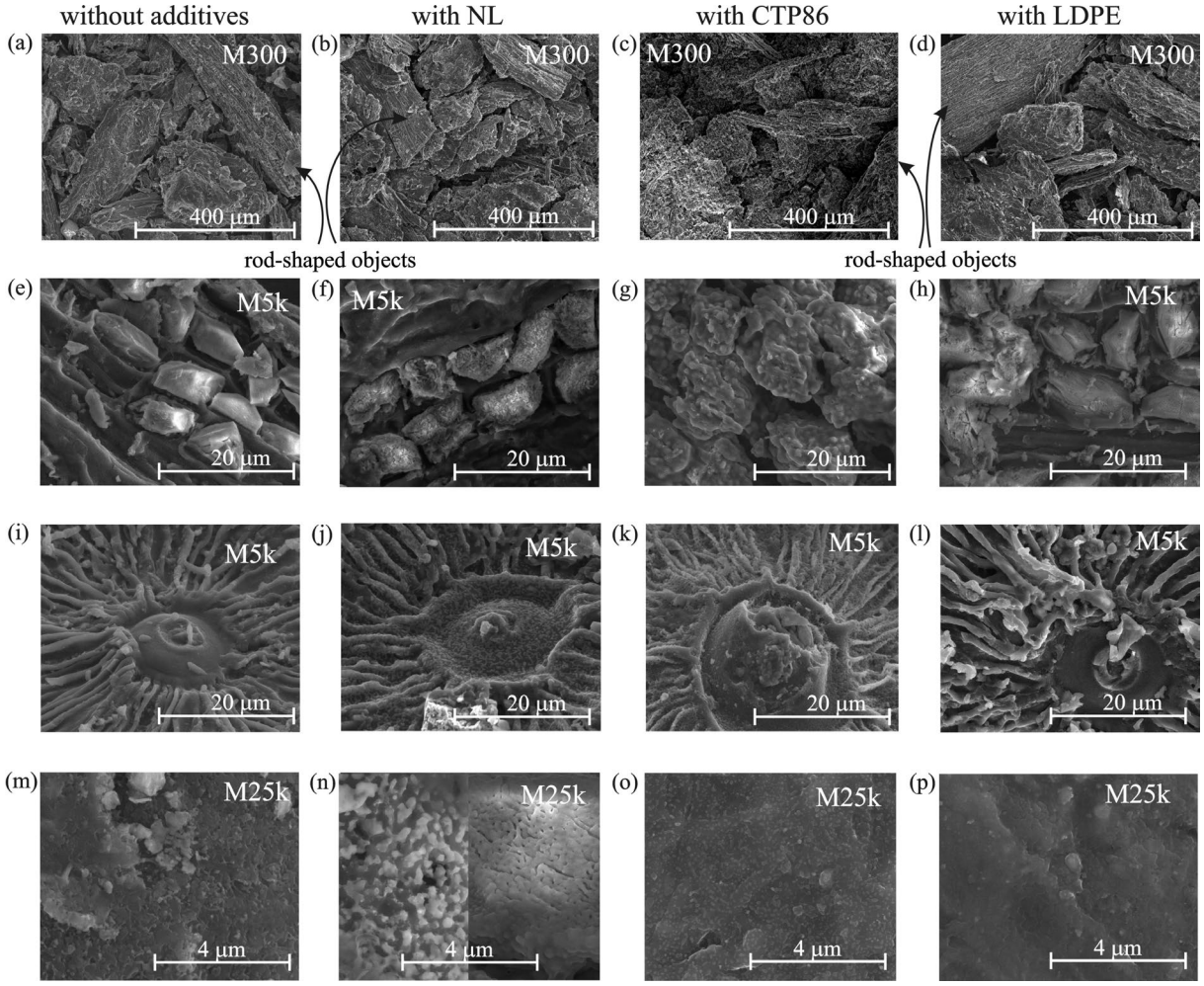

Figure 9. The SEM images of chars of densified PH sample and its blend with additives (**a**) char surface of PH; (**b**) char surface of PH with NL; (**c**) char surface of PH with CTP; (**d**) char surface of PH with LDPE; (**e**) 'bricks' in char from PH; (**f**) 'bricks' in char from PH with NL; (**g**) 'bricks' in char from PH with CTP; (**h**) 'bricks' in char from PH with LDPE; (**i**) 'star' in char from PH; (**j**) 'star' in char from PH with NL; (**k**) 'star' in char from PH with CTP; (**l**) 'star' in char from PH with LDPE; (**m**) flat surface of char from PH; (**n**) flat surface of char from PH with NL; (**o**) flat surface of char from PH with CTP; (**p**) flat surface of char from PH with LDPE.

On the flat surfaces of chars of pyrolysed samples, there are some visible characteristic reliefs similar to 'stars' with outgoing arms (Figure 9i–l). However, only in Figure 9j there are some deposits of lighter material visible on a 'star' from the blend of the PH sample with NL and on the surface of a 'star' from the blend of the PH sample with CTP there are some small pores that probably result from the loss of material of chars during gasification along with some deposits of lighter material. The EDX surface microanalysis of 'stars' in Table S3 shows the differences in composition of the areas of chars with 'stars'. Nevertheless, in these areas a greater amount of C, O, and K atoms is present.

Figure 9m–p present the SEM images of flat surfaces for chars at a magnification of M25k. The images show that all chars have a different surface relief. There are some areas with lighter deposits and some areas with the pores formed as a result of char gasification visible on the flat surface of chars from the PH sample with NL (Figure 9n). However, on the flat surface of char from the PH sample with CTP there are small deposits. The

EDX microanalysis of the surface presented in Table S3 shows that on these surfaces the amount of C atoms changes in the range of 35.60–49.13 wt%, that of O atoms changes in the range of 20.14–29.33 wt%, that of Mg atoms changes in the range of 1.85–4.13 wt%, that of P atoms changes in the range of 0.24–0.36 wt%, that of S atoms changes in the range of 0.41–0.79 wt%, that of Cl atoms changes in the range of 0.24–0.67 wt%, that of K atoms changes in the range of 23.03–32.23 wt%, and, finally, the amount of Ca atoms changes in the range of 1.84–3.19 wt%. The point microanalysis was conducted in order to explain the composition of lighter deposits that are visible in Figure 9n,j. The data presented in Figure S1 show that in the deposit material there are somehow reduced amounts of C (24.39 wt%), S (0.27 wt%), and K (16.50 wt%) atoms but somehow increased amounts of O (31.43 wt%), Mg (14.30 wt%), P (1.92 wt%), and Ca (9.57 wt%) atoms. Such a composition of deposits implies that the formation of Ca and Mg complexes with ligands originating from the volatile pyrolysis products of the PH sample is possible in the gas phase [46,48].

A different composition of inorganics in the studied chars can diversely catalyse the course of chemical reactions taking place during the co-pyrolysis of the PH sample with additives at pyrolysis temperatures above 450 °C and change the composition of volatile pyrolysis products along with the structure and composition of chars. A peak in the DTG curve (Figure 4) in the temperature range of 650–700 °C can be a proof of that. The differences in modification of the surface of inorganics by volatile products make the changed inorganics catalyse secondary reactions during char-volatile interactions in distinct ways.

4. Conclusions

The influence of LDPE, novolac, and coal tar pitch additives on the yield and composition of pyrolysis products from densified pea husks was studied. It was stated that all additives change the contribution ratio of saturated and unsaturated hydrocarbons, compounds with carbonyl groups, alcohols, phenols, and esters in the composition of volatile pyrolysis products from densified pea husks. The coal tar pitch additive causes the greatest reduction in these compounds in volatiles. All additives facilitate an increase in yield of the material condensable in methanol and in water. The greatest amount of the condensate soluble in methanol is obtained by the addition of LDPE, and that of the condensate soluble in water is obtained by the addition of coal tar pitch. The concentration of determined phenols and anhydrosugars slightly increases in water condensates under the influence of the additives. The additives to densified pea husks influence the yield of chars from the blends with additives, their structure, and composition. As a result of the interactions between the volatile pyrolysis products of the blends from pea husks with additives and the inorganics present in pea husks, new complex compounds having different compositions appear. The formed compounds can be the catalysers of chemical reactions taking place both in the gas phase and during the volatile-char interactions.

Supplementary Materials: The following supporting information can be downloaded at: https://www.mdpi.com/article/10.3390/en16062644/s1, Figure S1: The appearance of raw (**a**) and pyrolysed (**b**) tablets; Figure S2: The EDX point microanalysis of 'bricks'; Table S1: The mass of used tablets; Table S2: Concentration of selected phenols per 1 g sample [μg/L]; Table S3: Microanalysis results [wt%].

Author Contributions: Conceptualization, V.Z. and M.B.; methodology, V.Z. and M.B.; validation, V.Z., M.B. and A.S.; investigation, M.B., A.S. and V.Z.; resources, A.S.; data curation, M.B. and A.S.; writing—original draft preparation, V.Z. and M.B.; writing—review and editing, V.Z.; visualization, M.B., V.Z. and A.S.; supervision, V.Z.; project administration, V.Z.; funding acquisition, V.Z. All authors have read and agreed to the published version of the manuscript.

Funding: This research was funded by Jan Kochanowski University, grant number SUPB.RN.21.191.

Institutional Review Board Statement: Not applicable.

Informed Consent Statement: Not applicable.

Data Availability Statement: The data presented in this study are available on request from the corresponding author.

Acknowledgments: The authors would like thank A. Galuszka and J. Masternak for their help in obtaining the results of ultimate analysis and the analysis of composition of inorganics.

Conflicts of Interest: The authors declare no conflict of interest.

References

1. Pradhan, P.; Mahajani, S.M.; Arora, A. Production and utilization of fuel pellets from biomass: A review. *Fuel Process. Technol.* **2018**, *181*, 215–232. [CrossRef]
2. Rajput, S.P.; Jadhav, S.V.; Thorat, B.N. Methods to improve properties of fuel pellets obtained from different biomass sources: Effect of biomass blends and binders. *Fuel Process. Technol.* **2020**, *199*, 106255. [CrossRef]
3. Dai, X.; Theppitak, S.; Yoshikawa, K. Pelletization of carbonized wood using organic binders with biomass gasification residue as additive. *Energy Proc.* **2019**, *158*, 509–515. [CrossRef]
4. Espuelas, S.; Marcelino, S.; Echeverría, A.M.; del Castillo, J.M.; Seco, A. Low energy spent coffee grounds briquetting with organic binders for biomass fuel manufacturing. *Fuel* **2020**, *278*, 118310. [CrossRef]
5. Wang, T.; Tang, L.; Feng, X.; Xu, J.; Ding, L.; Chen, X. Influence of organic binders on the pyrolysis performance of rice straw pellets. *J. Anal. Appl. Pyrolysis* **2022**, *161*, 105366. [CrossRef]
6. Plaza, M.G.; Durán, I.; Rubiera, F.; Pevida, C. CO_2 adsorbent pellets produced from pine sawdust: Effect of coal tar pitch addition. *Appl. Energy* **2015**, *144*, 182–192. [CrossRef]
7. Cheng, J.; Zhou, F.; Si, T.; Zhou, J.; Cen, K. Mechanical strength and combustion properties of biomass pellets prepared with coal tar residue as a binder. *Fuel Process. Technol.* **2018**, *179*, 229–237. [CrossRef]
8. Ioannou, Z.; Simitzis, J. Production of carbonaceous adsorbents from agricultural by-products and novolac resin under a continuous countercurrent flow type pyrolysis operation. *Bioresour. Technol.* **2013**, *129*, 191–199. [CrossRef]
9. Faliagas, A.; Sfyrakis, J.; Simitzis, J. Influence of resin content on the sorption properties of adsorbents produced from novolac-biomass composites. *J. Mater. Sci.* **1996**, *31*, 199–203. [CrossRef]
10. Theodoropoulou, S.; Papadimitriou, D.; Zoumpoulakisa, L.; Simitzis, J. Optical properties of carbon materials formed by pyrolysis of novolac-resin/biomass composites. *Diam. Relat. Mater.* **2004**, *13*, 371–375. [CrossRef]
11. Hassan, H.; Hameed, B.H.; Lim, J.K. Co-pyrolysis of sugarcane bagasse and waste high-density polyethylene: Synergistic effect and product distributions. *Energy* **2020**, *191*, 116545. [CrossRef]
12. Ko, K.H.; Rawal, A.; Sahajwalla, V. Analysis of thermal degradation kinetics and carbon structure changes of co-pyrolysis between macadamia nut shell and PET using thermogravimetric analysis and ^{13}C solid state nuclear magnetic resonance. *Energy Convers. Manag.* **2014**, *86*, 154–164. [CrossRef]
13. Chen, W.; Shi, S.; Zhang, J.; Chen, M.; Zhou, X. Co-pyrolysis of waste newspaper with high-density polyethylene: Synergistic effect and oil characterization. *Energy Convers. Manag.* **2016**, *112*, 41–48. [CrossRef]
14. Zhou, H.; Meng, A.H.; Long, Q.Y.; Li, Q.H.; Zhang, Y.G. Interactions of municipal solid waste components during pyrolysis: A TG-FTIR study. *J. Anal. Appl. Pyrolysis* **2014**, *108*, 19–25. [CrossRef]
15. Jin, W.; Shen, D.; Liu, Q.; Xiao, R. Evaluation of the co-pyrolysis of lignin with plastic polymers by TG-FTIR and Py-GC/MS. *Polym. Degrad. Stab.* **2016**, *133*, 65–74. [CrossRef]
16. Xiong, S.; Zhuo, J.; Zhou, H.; Pang, R.; Yao, Q. Study on the co-pyrolysis of high density polyethylene and potato blends using thermogravimetric analyzer and tubular furnace. *J. Anal. Appl. Pyrolysis* **2015**, *112*, 66–73. [CrossRef]
17. Alam, M.; Bhavanam, A.; Jana, A.; Viroja, J.S.; Peela, N.R. Co-pyrolysis of bamboo sawdust and plastic: Synergistic effects and kinetics. *Renew. Energy* **2019**, *149*, 1133–1145. [CrossRef]
18. Zheng, Y.; Tao, L.; Yang, X.; Huang, Y.; Liu, C.; Zheng, Z. Study of the thermal behavior, kinetics, and product characterization of biomass and low-density polyethylene co-pyrolysis by thermogravimetric analysis and pyrolysis-GC/MS. *J. Anal. Appl. Pyrolysis* **2018**, *133*, 185–197. [CrossRef]
19. Hossain, M.S.; Ferdous, J.; Islam, M.S.; Islam, M.R.; Mustafi, N.N.; Haniu, H. Production of liquid fuel from co-pyrolysis of polythene waste and rice straw. *Energy Proc.* **2019**, *160*, 116–122. [CrossRef]
20. Lu, P.; Huang, Q.; (Thanos) Bourtsalas, A.C.; Chi, Y.; Yan, J. Synergistic effects on char and oil produced by the co-pyrolysis of pine wood, polyethylene and polyvinyl chloride. *Fuel* **2018**, *230*, 359–367. [CrossRef]
21. Yang, J.; Rizkiana, J.; Widayatno, W.B.; Karnjanakom, S.; Kaewpanha, M.; Hao, X.; Abudula, A.; Guanac, G. Fast co-pyrolysis of low density polyethylene and biomass residue for oil production. *Energy Convers. Manag.* **2016**, *120*, 422–429. [CrossRef]
22. Tang, Z.; Chen, W.; Chen, Y.; Yang, H.; Chen, H. Co-pyrolysis of microalgae and plastic: Characteristics and interaction effects. *Bioresour. Technol.* **2019**, *274*, 145–152. [CrossRef] [PubMed]
23. Xue, Y.; Kelkar, A.; Bai, X. Catalytic co-pyrolysis of biomass and polyethylene in a tandem micropyrolyzer. *Fuel* **2016**, *166*, 227–236. [CrossRef]
24. Kumagai, S.; Fujita, K.; Kameda, T.; Yoshioka, T. Interactions of beech wood-polyethylene mixtures during co-pyrolysis. *J. Anal. Appl. Pyrolysis* **2016**, *122*, 531–540. [CrossRef]
25. Dewangan, A.; Pradhan, D.; Singh, R.S. Co-pyrolysis of sugarcane bagasse and low-density polyethylene: Influence of plastic on pyrolysis product yield. *Fuel* **2016**, *185*, 508–516. [CrossRef]

26. Zubkova, V.; Strojwas, A. The influence of long-term storage on thermal behaviour of lower rank coal on the example of Polish coals. Part 2. The influence of expired ibuprofen (IB) and aspirin (AS) on changes in volume of long-term stored coal and on the composition of condensed material (CM) on the surface of grains. *Fuel* **2017**, *204*, 28–39. [CrossRef]
27. Zubkova, V.; Strojwas, A.; Kaniewski, M.; Jany, B.R. The influence of the additives of expired paracetamol (PR) and naproxen (NP) on the thermal behaviour of high volatile bituminous coal (HVBC) and the composition of material extracted from the zones of its plastic layer. *Fuel* **2020**, *273*, 117752. [CrossRef]
28. Bielecki, M.; Zubkova, V.; Strojwas, A. Influence of Densification on the Pyrolytic Behavior of Agricultural Biomass Waste and the Characteristics of Pyrolysis Products. *Energies* **2022**, *15*, 4257. [CrossRef]
29. Czaplicka, M.; Cieślik, E.; Komosiński, B.; Rachwał, T. Emission Factors for Biofuels and Coal Combustion in a Domestic Boiler of 18 kW. *Atmosphere* **2019**, *10*, 771. [CrossRef]
30. Janoszka, K.; Czaplicka, M.; Klejnowski, K. Comparison of biomass burning tracer concentrations between two winter seasons in Krynica Zdrój. *Air Qual. Atmos. Health* **2020**, *13*, 379–385. [CrossRef]
31. Fushimi, C.; Katayama, S.; Tsutsumi, A. Elucidation of interaction among cellulose, lignin and xylan during tar and gas evolution in steam gasification. *J. Anal. Appl. Pyrolysis* **2009**, *86*, 82–89. [CrossRef]
32. Hilbers, T.J.; Wang, Z.; Pecha, B.; Westerhof, R.J.M.; Kersten, S.R.A.; Pelaez-Samaniego, M.R.; Garcia-Pereza, M. Cellulose-Lignin interactions during slow and fast pyrolysis. *J. Anal. Appl. Pyrolysis* **2015**, *114*, 197–207. [CrossRef]
33. Liu, Q.; Zhong, Z.; Wang, S.; Luo, Z. Interactions of biomass components during pyrolysis: A TG-FTIR study. *J. Anal. Appl. Pyrolysis* **2011**, *90*, 213–218. [CrossRef]
34. Wu, S.; Shen, D.; Hu, J.; Zhang, H.; Xiao, R. Cellulose-hemicellulose interactions during fast pyrolysis with different temperatures and mixing methods. *Biomass Bioenergy* **2016**, *95*, 55–63. [CrossRef]
35. Hu, J.; Jiang, B.; Liu, J.; Sun, Y.; Jiang, X. Influence of interactions between biomass components on physicochemical characteristics of char. *J. Anal. Appl. Pyrolysis* **2019**, *144*, 104704. [CrossRef]
36. Traoré, M.; Kaal, J.; Martínez Cortizas, A. Application of FTIR spectroscopy to the characterization of archeological wood. *Spectrochim. Acta A* **2016**, *153*, 63–70. [CrossRef]
37. Zubkova, V.; Strojwas, A.; Bielecki, M.; Kieush, L.; Koverya, A. Comparative study of pyrolytic behavior of the biomass wastes originating in the Ukraine and potential application of such biomass. Part 1. Analysis of the course of pyrolysis process and the composition of formed products. *Fuel* **2019**, *254*, 115688. [CrossRef]
38. Rocha, M.V.; Vinuesa, A.J.; Pierella, L.B.; Renzini, M.S. Enhancement of bio-oil obtained from co-pyrolysis of lignocellulose biomass and LDPE by using a natural zeolite. *Therm. Sci. Eng. Prog.* **2022**, *19*, 100654. [CrossRef]
39. Marcilla, A.; Gómez-Siurana, A.; Valdés, F. Catalytic cracking of low-density polyethylene over H-Beta and HZSM-5 zeolites: Influence of the external surface. Kinetic model. *Polym. Degrad. Stab.* **2007**, *92*, 197–204. [CrossRef]
40. Dubdub, I.; Al-Yaari, M. Pyrolysis of Low Density Polyethylene: Kinetic Study Using TGA Data and ANN Prediction. *Polymers* **2020**, *12*, 891. [CrossRef]
41. Yang, H.; Liu, M.; Chen, Y.; Xin, S.; Zhang, X.; Wang, X.; Chen, H. Vapor-solid interaction among cellulose, hemicellulose and lignin. *Fuel* **2020**, *263*, 116681. [CrossRef]
42. Song, Y.; Wang, Y.; Hu, X.; Hu, S.; Xiang, J.; Zhang, L.; Zhang, S.; Min, Z.; Li, C.Z. Effects of volatile-char interactions on in situ destruction of nascent tar during the pyrolysis and gasification of biomass. Part I. Roles of nascent char. *Fuel* **2014**, *122*, 60–66. [CrossRef]
43. Gao, A.; Wang, Y.; Lin, G.; Li, B.; Hu, X.; Huang, Y.; Zhang, S.; Zhang, H. Volatile-char interactions during biomass pyrolysis: Reactor design toward product control. *Renew. Energy* **2022**, *185*, 1–7. [CrossRef]
44. Hosoya, T.; Kawamoto, H.; Saka, S. Solid/liquid- and vapor-phase interactions between cellulose- and lignin-derived pyrolysis products. *J. Anal. Appl. Pyrolysis* **2009**, *85*, 237–246. [CrossRef]
45. Chen, Y.; Fang, Y.; Yang, H.; Xin, S.; Zhang, X.; Wang, X.; Chen, H. Effect of volatiles interaction during pyrolysis of cellulose, hemicellulose, and lignin at different temperatures. *Fuel* **2019**, *248*, 1–7. [CrossRef]
46. Song, Y.; Wang, Y.; Hu, X.; Xiang, J.; Hu, S.; Mourant, D.; Li, T.; Wu, L.; Li, C.Z. Effects of volatile-char interactions on in-situ destruction of nascent tar during the pyrolysis and gasification of biomass. Part II. Roles of steam. *Fuel* **2015**, *143*, 555–562. [CrossRef]
47. Cieślak-Golonka, M.; Starosta, J.; Wasilewski, M. *Introduction to Coordination Chemistry*, 2nd ed.; Scientific Publishing House PWN SA: Warsaw, Poland, 2013; pp. 158–184. (In Polish)
48. Bielański, A. *Fundamentals of Inorganic Chemistry*, 2nd ed.; Academic Publishing PWN: Warsaw, Poland, 1994; pp. 720–721. (In Polish)
49. Shen, Y.; Yu, S.; Yuan, R.; Wang, P. Biomass pyrolysis with alkaline-earth-metal additive for co-production of bio-oil and biochar-based soil amendment. *Sci. Total Environ.* **2020**, *743*, 140760. [CrossRef]
50. Cotton, F.A.; Wilkinson, G.; Gaus, P.L. *Basic Inorganic Chemistry*; Scientific Publishing House PWN SA: Warsaw, Poland, 1998; pp. 331–332. (In Polish)
51. Huang, F.; Li, S.; Song, J.; Chen, L.; Zhang, X.; Shen, Y.; Xie, A. Complex calcium carbonate aggregates: Controlled crystallization and assembly via an additive-modified positive-microemulsion-route. *CrystEngComm* **2012**, *14*, 1277–1282. [CrossRef]